VTT Technical Research Centre of Finland

Driving a low critical current Josephson junction array with a mode-locked laser

Nissilä, Jaani; Fordell, Thomas; Kohopää, Katja; Mykkänen, Emma; Immonen, Pirjo; Jabradaghi, Robab Najafi; Bardalen, E.; Kieler, O.; Karlsen, B.; Ohlckers, P. A.; Behr, R.; Manninen, Antti J.; Govenius, Joonas; Kemppinen, Antti

Published in:
Applied Physics Letters

DOI:
10.1063/5.0060804

Published: 21/07/2021

Document Version
Publisher's final version

Applied Physics Letters

Driving a low critical current Josephson junction array with a mode-locked laser

Cite as: Appl. Phys. Lett. **119**, 032601 (2021); https://doi.org/10.1063/5.0060804
Submitted: 22 June 2021 . Accepted: 22 June 2021 . Published Online: 21 July 2021

J. Nissilä, T. Fordell, K. Kohopää, E. Mykkänen, P. Immonen, R. N. Jabdaraghi, E. Bardalen, O. Kieler, B. Karlsen, P. A. Øhlckers, R. Behr, A. J. Manninen, J. Govenius, and A. Kemppinen

Applied Physics Letters ARTICLE scitation.org/journal/apl

Driving a low critical current Josephson junction array with a mode-locked laser

Cite as: Appl. Phys. Lett. **119**, 032601 (2021); doi: 10.1063/5.0060804
Submitted: 22 June 2021 · Accepted: 22 June 2021 ·
Published Online: 21 July 2021

View Online Export Citation CrossMark

J. Nissilä,[1,a)] T. Fordell,[1] K. Kohopää,[1] E. Mykkänen,[1] P. Immonen,[1] R. N. Jabdaraghi,[1] E. Bardalen,[2] O. Kieler,[3] B. Karlsen,[4] P. A. Øhlckers,[2] R. Behr,[3] A. J. Manninen,[1] J. Govenius,[1] and A. Kemppinen[1]

AFFILIATIONS

[1]VTT Technical Research Centre of Finland Ltd, 02150 Espoo, Finland
[2]University of South-Eastern Norway, 3184 Borre, Norway
[3]Physikalisch-Technische Bundesanstalt (PTB), 38116 Braunschweig, Germany
[4]Justervesenet, 2007 Keller, Norway

[a)]Author to whom correspondence should be addressed: Jaani.Nissila@vtt.fi

ABSTRACT

We report proof-of-concept experiments on an optically driven Josephson voltage standard based on a mode-locked laser (MLL), a time-division multiplexer, and a cryogenic ultrafast photodiode driving an overdamped Josephson junction array (JJA). Our optical pulse pattern generator (PPG) concept builds on the capability of MLLs to produce trains of picosecond-wide optical pulses with little amplitude and temporal spread. Our present setup enables multiplication of the original 2.3 GHz pulse repetition frequency by a factor of 8. A commercial photodiode converts the optical pulses into about 25 ps wide electrical pulses in liquid helium several cm from the JJA. Using a custom-made MLL, we can drive a JJA with a low critical current of 360 μA at multiple Shapiro steps. We have performed experiments with pulse pairs whose time interval can be set freely without distorting the shapes of individual pulses. Experimental results are in qualitative agreement with theoretical simulations, and they demonstrate, e.g., crossover in the Shapiro step pattern when the time interval between the pulses is approximately equal to the inverse of the characteristic frequency of the JJA. However, there are quantitative discrepancies, which motivate an improved integration of photodiodes and JJAs to improve both the understanding and fidelity of Josephson Arbitrary Waveform Synthesizers. Considering future quantum technologies in a wider perspective, our optical approach is a potential enabler for fast and energy-efficient pulse drive without an expensive high-bandwidth electrical PPG and without high-bandwidth electrical cables that yield too high thermal conductance between cryogenic and room temperatures.

Three types of Josephson voltage standards (JVS)[1–5] are commonly used for voltage metrology: (i) hysteretic Josephson junction arrays (JJA) are considered most reliable for dc voltage at ultimate precision, but their operation can require manual labor. (ii) Programmable non-hysteretic JJAs allow automated dc and low-frequency ac measurements, but their accuracy suffers from non-quantized transient periods[6–9] and ground currents due to the complex biasing circuitry.[10–12] (*iii*) Josephson Arbitrary Waveform Synthesizer (JAWS) driven with ultrafast current pulses can generate arbitrary waveforms,[13] but technical challenges have limited their maximum output voltage to well below 10 V, which would be required for practical metrology.[14–17]

In this Letter, we utilize optical pulse generation to pave the way for establishing JAWS as the only required JVS. Conventional JAWS is driven with electrical pulse pattern generators (PPG) and coaxial transmission lines between room temperature (RT) and cryogenic temperature. When aiming at higher pulse rates to enable higher voltages and frequencies, electrical cables have a problematic trade-off: they either conduct too much heat or have too low bandwidth. To overcome this bottleneck, a promising possibility is to use optical pulse patterns and ultrafast photodiodes (PD) at 4 K to drive JJAs.[18,19] A similar technique was recently used for the control and readout of superconducting qubits, since thermal loading through electrical cabling hinders scalability of quantum computing.[20] In this field, also inherent distortions in metallic coaxial cables can cause difficulties.[21] With JAWS, robust mounting techniques for the PDs at 4 K[22,23] enabled the demonstration of quantized voltage waveforms using pulse rates up to several GHz.[24,25] All these experiments relied on controlling the intensity of continuous-wave (CW) light with optical intensity modulators (OIM) and expensive high-frequency electronics.

In our proof-of-concept experiments, we generate the optical pulses with a mode-locked laser (MLL) and an optical time-division multiplexer (TDM). They enable picosecond pulses with very little amplitude variation and time jitter,[26,27] which is challenging using CW light and OIMs driven by electronic PPGs but would be useful for future high-speed JAWS.[28] Our vision is to develop an optical PPG, which could be used, e.g., together with ultrafast uni-travelling-carrier PDs[29,30] to increase the maximum pulse frequency that drives Josephson junction circuits. Here, we use fast commercial PDs[31] to demonstrate that the performance of our custom-made MLL is sufficient for driving a JJA with low critical current (I_c) at multiple Shapiro steps. We study the response of the JJA to direct current and simple current pulse pairs to develop the understanding of the system as a whole, especially to understand the future requirements for more advanced JAWS.

A JJA quantizes electric pulse patterns such that the voltage across the array equals $V(t) = Ns(t) \times \frac{h}{2e} f(t)$.[2–4] Here, N is the number of junctions in series, s is an integer describing the Shapiro step index to which the array is biased at time t, $f(t)$ is the time-dependent pulse frequency, and $h/(2e)$ is the magnetic flux quantum, where h is the Planck constant and e is the elementary charge. When aiming at increased voltages, an evident possibility is to use higher pulse rates or higher Shapiro steps, or both. The latter is easier for JJAs with low I_c since they allow smaller magnitude of the current pulses, which decreases heat dissipation and improves the linearity of PDs.[32] However, if I_c is too low, the Josephson coupling energy and the shot noise of the PD may become limitations. We focus on a JJA with $I_c = 360\ \mu$A, which is considerably lower than in typical JAWS.[5] For reference, we also use another JJA with higher I_c.

Figure 1(a) shows the basic structure of our optical PPG concept. The MLL produces fast pulses in the wavelength range from 1200 to 1700 nm at a modest repetition rate of 1–10 GHz. The TDM splits the parent pulses into several waveguides without introducing additional noise. Each path has an OIM that is used either to pass or block pulses. Modulator state transitions are arranged to happen almost simultaneously and well before the arrival of pulses, enabling negligible distortion to the passing pulses. The pulses are subsequently interleaved with proper delays and combined back to a single waveguide. Figure 1(b) illustrates an example of pulse pattern evolution in a system, which enables multiplication of the MLL pulse repetition rate f_{MLL} by a factor of 4. As discussed in supplementary material A, a relative jitter below 10^{-6} in instantaneous pulse frequency is feasible at a multiplied pulse rate up to 40 GHz.

Figure 1(c) illustrates our proof-of-concept experiment. We have built an inexpensive MLL at 1335 nm wavelength, which is suitable for generating charge carriers in regular InGaAs photodiode at 4.2 K. The pulse repetition rate was set to $f_{MLL} = 2.3$ GHz. The laser uses hybrid mode-locking in a ring cavity: the pulsing is excited using both a semiconducting saturable absorber mirror and by varying the gain of a semiconducting optical amplifier (SOA) with a microwave generator. The transform-limited pulse duration (full width at half maximum, FWHM) of our laser pulses is about 6 ps, but the 20 GHz p–i–n photodiode[31] broadens the current pulses to approximately 25 ps in this experiment. The MLL pulses are further amplified with an SOA[33] and guided into the TDM, which is composed of fiber-optic splitters and four adjustable free-space delay lines. SOAs in our setup increase the optical power to a sufficient level for the JJAs. They are commercial single-pass booster amplifiers with high saturation output power above +15 dBm.[33]

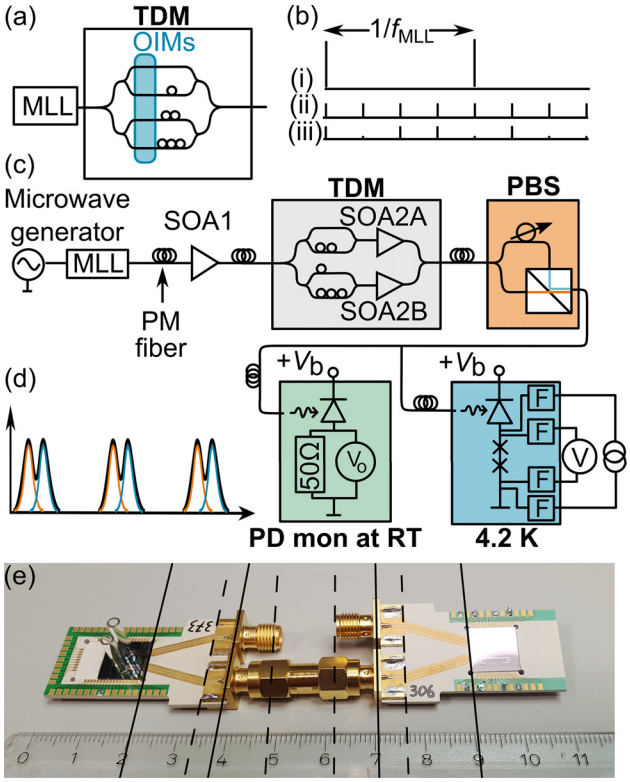

FIG. 1. (a) Simplified illustration of an optical pulse pattern generator with a mode-locked laser (MLL), time-division multiplexer (TDM), and optical intensity modulators (OIM) for pulse picking. (b) An example of the pulse pattern at (i) the MLL, (ii) the TDM output when modulators pass all pulses, and (iii) the TDM output when some pulses are blocked. (c) A more detailed diagram of the PPG used in this paper. SOAxx: semiconducting optical amplifiers; PD mon: monitoring photodiode; PBS: polarization based splitter; F: low-pass filter. (d) Illustration of two pulses with orthogonal polarizations (blue and orange) summed by the PBS to form a composite pulse. (e) Photograph of the cryogenic assembly with PD on the left with a glass tube for fiber mounting, and standard JAWS carrier and chip setup with SMA connector on the right. The solid and dashed lines show possible non-ideal mismatched interfaces in the high-speed transmission line of this preliminary experimental setup.

Our optical PPG does not yet have OIMs, but we can test the JAWS-like operation by blocking some of the optical paths. In addition, we have a polarization-based splitter (PBS) that can increase the maximum pulse frequency by a factor of 2 leading to $2 \times 4 \times 2.3\ \text{GHz} = 18.4\ \text{GHz}$. The PBS splits the incoming linearly polarized pulses into two beams with orthogonal polarizations before combining them again. Both time interval Δt and the amplitudes of the pulses can be set to any values without distorting the shape of individual pulses. The pulses can even be set overlapping without interference induced instabilities.

The optical pulses are brought to the PD at 4 K with a polarization maintaining (PM) single-mode fiber, which can be considered a distortion-free media for the pulses and does not conduct heat significantly. The PD carrier and the JJA are mounted on separate printed

circuits boards connected together with a 3.5 mm connector [Fig. 1(e)]. We also split the optical pulses to a similar PD at RT to monitor the output pulses approximately with an oscilloscope.

The thermal load that the optical drive causes is directly proportional to the pulsed photocurrent I_{Photo} and the voltage across the photodiode depletion region. We estimate the dissipated power as $P_{tot} = I_{Photo} \times (1/r + U_{RB} + U_{BI})$, where r is the responsivity of the PD, U_{RB} is the external reverse bias voltage, and U_{BI} is the built-in voltage of the PD (see supplementary material B). The pulsed current depends directly on the I_c of the JJs, and thereby, the reduction in I_c is beneficial from the thermal point of view, too.

We measure two superconductor–normal metal–superconductor (SNS) type JJAs fabricated at PTB. They have $N = 1000$ Nb-Nb_xSi_{1-x}-Nb Josephson junctions in series along the center conductor of a wideband superconducting coplanar waveguide (CPW).[34,35] Array A has $I_c = 360\,\mu$A and junction resistance $R_J = 30.8$ m Ω, which yield the characteristic frequency[13] $f_c = 5.4$ GHz. For comparison, array B has markedly different properties, such as $I_c = 2.3$ mA, $R_J = 11.4$ m Ω, and $f_c = 12.7$ GHz. To compensate the dissipation of the JJA the insulating gap of the CPW narrows down linearly so that the transmission line impedance decreases from 50 to 35 Ω.[36] The ideal impedance at the end of the array would be $50\,\Omega - NR_J$, i.e., 19 and 39 Ω for arrays A and B, respectively. More details on the experimental setup can be found in supplementary material C and Refs. 22, 23, and 25.

In the experiments, we use the TDM and the PBS [Fig. 1(c)] to generate pulse pairs with a variable Δt at a repetition rate of 2.3 GHz. The amplitude of the pulse pair is tuned by the amplification of SOA1. We repeat the same pulse pattern many times and use the average voltage as a function of Δt, pulse amplitude, and dc current to detect deviations from ideal performance. Such effects can be detrimental for high-frequency JAWS where Δt is small.

Figure 2 presents the experimental and simulated average voltage of array A with five different values of Δt, varying from 30 to 220 ps [see panel (g)]. Panels (a)–(f) show the results for normalized voltage $v = V/\left(N \times \frac{h}{2e} \times f_{MLL}\right)$ as a function of normalized pulse integral p and supplementary dc bias current I_{dc}. We define $p = \frac{2\pi f_c}{I_c} \int_0^{1/f_{MLL}} I_p(t)\mathrm{d}t$, where $I_p(t) = I(t) - I_{dc}$ is the pulse current. At the quantized voltage plateaus, v is ideally an integer $v = s \times m$, where m is the number of pulses in the period $1/f_{MLL}$ (in our case $m = 2$). The simulations of panels (b), (d), and (f) were performed with a single junction model (resistively and capacitively shunted junction, RCSJ) that omits transmission line effects[37,38] (see supplementary material D.1).

The characteristic time for array A is $t_c = 1/f_c = 190$ ps. For $\Delta t > t_c$, the JJA has sufficient time to recover after each pulse, and we see quantized plateaus only with even $v = 0, 2, 4, \ldots$ In the opposite limit, $\Delta t \ll t_c$, the JJA sees the two pulses as a single one with $p = p_1 + p_2$, where p_1 and p_2 are the integrals of the individual current pulses. In this limit, we see all plateaus $v = 1, 2, 3, \ldots$ For intermediate Δt, we also see all plateaus, but ones with even index are wider than those with odd index. The results of our measurements and single-junction simulations are in qualitative agreement. Note that the voltage maps in Fig. 2 were not measured aiming at verification of flatness of quantized levels. However, with Array B we measured step ($v = 2$) flatness with parts per million precision giving us confidence on the sufficient quality of PPG pulse trains for driving JJAs.

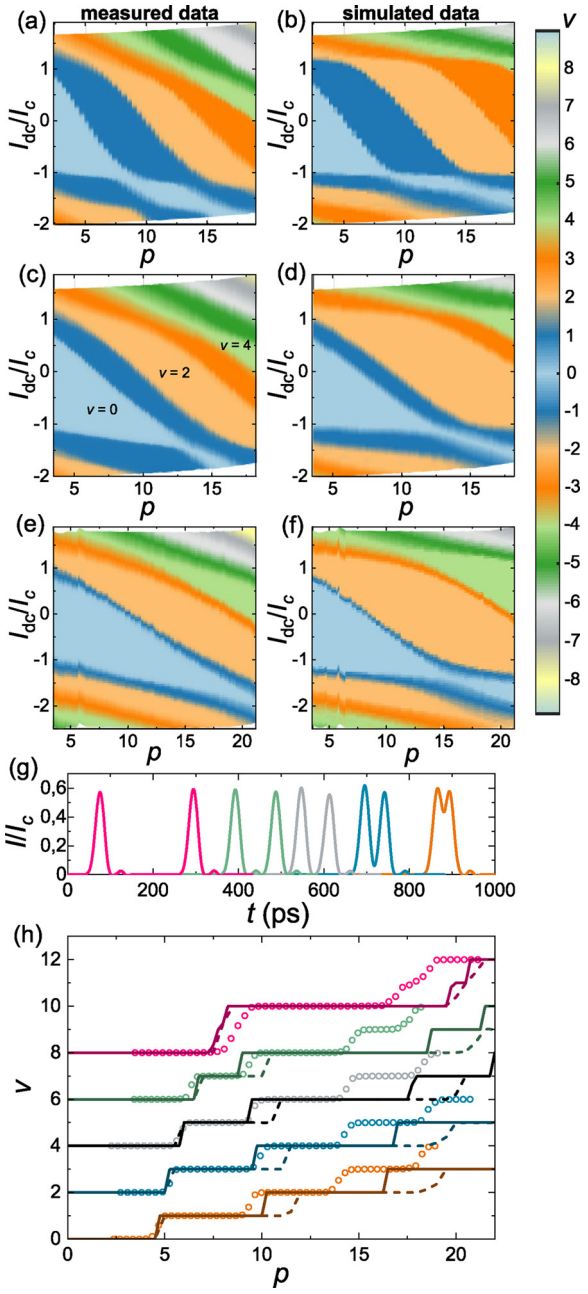

FIG. 2. (a)–(f) Measured and simulated average JJA voltage as a function of normalized current pulse time-integral and normalized dc current through the array. Current pulse pairs with the repetition rate of 2.3 GHz (period 430 ps) with time intervals Δt of 30 [(a) and (b)], 95 [(c) and (d)], and 220 ps [(e) and (f)] were applied. (g) Current pulse patterns composed of two elementary pulses set at different time intervals from each other: 30 ps (orange), 45 ps (blue), 70 ps (gray), 95 ps (green), and 220 ps (red). These pulse patterns are based on measurements using a monitoring photodiode at room temperature. (h) Comparison of measured and simulated average voltages at zero dc current as a function of normalized pulse integral. The circles depict the experimental values, the solid lines show the simulated results using a single-JJ model, and the dashed lines show the simulated values using a transmission line model for the JJA (1000 JJ) and an unterminated photodiode in a 10 mm long 50 Ω transmission line. Different traces correspond to different Δt with the same colors as in (g), and they have been shifted vertically for clarity.

In the following discussion, we concentrate on the $I_{dc} = 0$ data shown in Fig. 2(h). We scale the pulse integral data measured from the room temperature monitor PD [Fig. 2(g)] with a single fitting parameter. It is chosen such that the measured transition from $v = 0$ to $v = 1$ with $\Delta t = 30$ ps occurs at the same pulse integral as the simulated transition.

Measured transitions between Shapiro steps are sharp thanks to the low noise of the optical pulses. The single-JJ simulations predict that the width of even plateaus increases with the increasing Δt, but this effect is significantly weaker in the measured data. In particular, the measured plateau $v = 2$ (corresponding to $V \approx 9.5$ mV) has nearly equal width for all values from $\Delta t = 30$ to $\Delta t = 95$ ps. However, thanks to the adjustability of the Δt between the short pulses, we can observe experimentally the crossover at $\Delta t = t_c$: as expected, odd steps are missing with the longest $\Delta t = 220$ ps $> t_c$, but they are observable when $\Delta t < t_c$.

Qualitatively similar observations, i.e., that plateaus with odd v are wider than expected for $\Delta t \approx 100$ ps, were also obtained experimentally for array B (data not shown). Since it had a notably shorter characteristic time $t_c = 80$ ps, it is clear that the simple model cannot explain our results. The RCSJ model omits the heating of the JJs, which is essentially proportional to $R_J\langle I^2\rangle$ where $\langle I^2\rangle$ is the time average of the total current squared through the junction. Heating is, thus, much more significant in array B that has a larger I_c. We cannot overrule heating effects at the highest Shapiro steps and dc currents, but the qualitative similarity of results between arrays A and B also indicates that heating does not explain the discrepancy between experiments and single-JJ simulations.

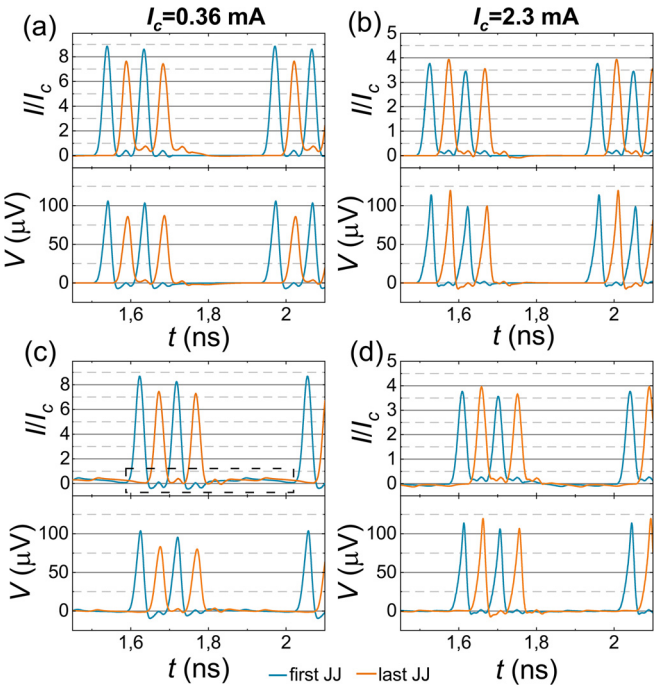

FIG. 3. Simulated current pulse waveforms through and voltage pulse waveforms across the first and last JJ in a JJA for arrays A and B with two pulses separated by 95 ps. Panels (a)–(b) show the simulated current and voltage for the case without any transmission line between PD and JJA for arrays A and B, respectively. Panels (c)–(d) show the corresponding simulations when there is a 10 mm transmission line between PD and JJA. The simulations shown here were performed in the middle of plateau $v = 2$. Note the amplitude of current fluctuation $I_c/2$ in the background (dashed box).

To obtain more insight into the system, we have built a transmission line model for the whole JJA (see supplementary material D.2). The PD is modeled as an ideal current source and the JJA is terminated with a 35 Ω resistor. In our first simple model, the PD is directly connected to the first junction of the JJA. Considering the data in Fig. 2, the single-JJ and transmission line models agree with minor differences.

In pulse-waveform simulations of Fig. 3, we have used a more realistic but still over-simplified model for our highly non-ideal connection between the PD and the JJA [see Fig. 1(e)]: 10 mm of ideal 50 Ω passive transmission line. Such a distance may be realistically required, e.g., to avoid overheating of JJs during gold-based flip-chip-bonding of the PD on a JJA chip. Any non-ideality of the JJA transmission line will reflect part of the drive pulses back to the PD. Since the PD has a high impedance, most of the energy reflects back to the JJA.

In Fig. 3, the simulation results for the first and last JJ of arrays A and B correspond to a quasi-steady state in the middle of plateau $v = 2$. Current and voltage are periodic with repetition time $1/f_{MLL}$. Current pulse reflections enhanced by the passive transmission line cause both rapidly time-varying and period-long fluctuations in current background, with the magnitude of the order of $I_c/2$ in panel (c). Reflections are stronger in array A than B that we relate to the less ideal impedance matching. We interpret that such reflections are the reason for the disagreement between experiments and single-junction simulations of Fig. 2 and have a significant effect on the position of quantized voltage plateaus [dashed lines in Fig. 2(h)]. Note that the magnitude of background current fluctuations may increase with the increasing p, which yields a non-trivial distortion of the voltage maps shown in Fig. 2.

In our simulations, we have also observed erroneous events where the response of the JJA to a pulse depends on the history of the preceding pulses as a result of unsettled current background. This emphasizes the importance of transmission line optimization for the correct operation of JAWS.

Based on the measured pulse current through the PD and JJA and the simulation results, we believe that in our actual setup nearly 30% of the pulse current spreads in the background, likely unevenly. That background current is a possible origin of the disagreement between experimental and simulated data and can lead to a shift of the voltage plateaus in Fig. 2(h) into either direction on the p axis.

To conclude, we report proof-of-concept studies of an optically driven Josephson voltage standard based on generating fast optical pulses with a mode-locked laser. Voltage quantization takes place using a JJA with a relatively low critical current $I_c = 360$ μA. Temporal performance analyses of optical PPG and sharp transitions between Shapiro steps indicate, correspondingly, that both timing jitter and amplitude noise of the optical pulses are sufficiently low for the metrological operation of the JJA. However, comparison between measurements and simulations shows that in the future, the PD should be mounted close to a JJA, and the PD should possibly be matched to the transmission line with a resistive shunt. To summarize, our results pave the way for using higher Shapiro steps and higher pulse frequencies to obtain higher output

voltages with JAWS with no identified fundamental limitations, but practical optimization of especially the JJAs still required. Reduced thermal loading is expected to enable efficient drive of multiple JJAs.

See the supplementary material for an analysis of the temporal performance of the optical pulse pattern generator concept (supplementary material A), analysis of the heat load caused by the optical drive (supplementary material B), further details of the experimental setup (supplementary material C), and a description of the simulation methods of JJA (supplementary material D).

We acknowledge fruitful discussions with Dr. Mikko Merimaa from VTT in the beginning of the PPG concept development. We also thank Dr. Mark Bieler and Dr. Luis Palafox from PTB for discussions. We acknowledge the Academy of Finland for support through Grant Nos. 310909, 296476 (T.F.), and 306844 (T.F.). This work is also part of the Academy of Finland Flagship Programme, Photonics Research and Innovation (PREIN), decision 320168. This work has also received funding from the European Union's Horizon 2020 Research and Innovation Programme under the QuADC project of the EMPIR program and Grant Agreement No. 862660/Quantum e-leaps. We also acknowledge funding from an internal strategic innovation project of VTT related to the development of quantum computing technologies.

DATA AVAILABILITY

The data that support the findings of this study are available from the corresponding author upon reasonable request.

REFERENCES

[1]B. D. Josephson, Phys. Lett. **1**, 251 (1962).
[2]C. A. Hamilton, Rev. Sci. Instrum. **71**, 3611 (2000).
[3]J. Kohlmann, R. Behr, and T. Funk, Meas. Sci. Technol. **14**, 1216 (2003).
[4]B. Jeanneret and S. P. Benz, Eur. Phys. J. Spec. Top. **172**, 181 (2009).
[5]A. Rüfenacht, N. E. Flowers-Jacobs, and S. P. Benz, Metrologia **55**, S152 (2018).
[6]J. Lee, R. Behr, A. S. Katkov, and L. Palafox, IEEE Trans. Instrum. Meas. **58**, 803 (2009).
[7]B. Jeanneret, F. Overney, A. Rufenacht, and J. Nissila, "Strong attenuation of the transients' effect in square waves synthesized with a programmable Josephson voltage standard," IEEE Trans. Instrum. Meas. **59**, 1894–1899 (2010).
[8]C. J. Burroughs, A. Rüfenacht, S. P. Benz, P. D. Dresselhaus, B. C. Waltrip, and T. L. Nelson, IEEE Trans. Instrum. Meas. **57**, 1322 (2008).
[9]C. J. Burroughs, A. Rüfenacht, S. P. Benz, and P. D. Dresselhaus, IEEE Trans. Instr. Meas. **58**, 761 (2009).
[10]S. Solve, A. Rüfenacht, C. J. Burroughs, and S. P. Benz, Metrologia **50**, 441 (2013).
[11]S. Solve, R. Chayramy, A. Rüfenacht, C. J. Burroughs, and S. P. Benz, "The leakage resistance to ground of a NIST programmable Josephson voltage standard," in *the 29th Conference on Precision Electromagnetic Measurements (CPEM 2014)*, Rio de Janeiro, Brazil (IEEE, 2014), pp. 462–463.
[12]A. Rüfenacht, C. J. Burroughs, P. D. Dresselhaus, and S. P. Benz, "Measurement of leakage current to ground in programmable Josephson voltage standards," in *2018 Conference on Precision Electromagnetic Measurements (CPEM 2018), Paris France* (IEEE, 2018), pp. 1–2.
[13]S. P. Benz and C. A. Hamilton, Appl. Phys. Lett. **68**, 3171 (1996).
[14]O. F. Kieler, R. Behr, R. Wendisch, S. Bauer, L. Palafox, and J. Kohlmann, IEEE Trans. Appl. Supercond. **25**, 14003051 (2015).
[15]S. P. Benz, S. B. Waltman, A. E. Fox, P. D. Dresselhaus, A. Rüfenacht, J. M. Underwood, L. A. Howe, R. E. Schwall, and C. J. Burroughs, Jr., "One-volt Josephson arbitrary waveform synthesizer," IEEE Trans. Appl. Supercond. **25**, 1300108 (2015).
[16]N. E. Flowers-Jacobs, A. Rüfenacht, A. E. Fox, S. B. Waltman, J. A. Brevik, P. D. Dresselhaus, and S. P. Benz, "Three volt pulse-driven Josephson arbitrary waveform synthesizer," in *2018 Conference on Precision Electromagnetic Measurements (CPEM 2018), Paris, France* (IEEE, 2018), pp. 1–2.
[17]N. E. Flowers-Jacobs, A. Rüfenacht, A. E. Fox, P. D. Dresselhaus, and S. P. Benz, in 2020 Conference on Precision Electromagnetic Measurements (CPEM 2020), Denver, CO, USA (IEEE, 2020), pp. 1–2.
[18]C. Urano, N. Kaneko, M. Maezawa, T. Itatani, and S. Kiryu, J. Phys.: Conf. Ser. **97**, 012269 (2008).
[19]J. Williams, T. J. B. M. Janssen, L. Palafox, D. A. Humphreys, R. Behr, J. Kohlmann, and F. Müller, Supercond. Sci. Technol. **17**, 815 (2004).
[20]F. Lecocq, F. Quinlan, K. Cicak, J. Aumentado, S. A. Diddams, and J. D. Teufel, Nature **591**, 575 (2021).
[21]M. A. Rol, L. Ciorciaro, F. K. Malinowski, B. M. Tarasinski, R. E. Sagastizabal, C. C. Bultink, Y. Salathe, N. Haandbaek, J. Sedivy, and L. DiCarlo, Appl. Phys. Lett. **116**, 054001 (2020).
[22]E. Bardalen, B. Karlsen, H. Malmbekk, O. Kieler, M. N. Akram, and P. Ohlckers, IEEE Trans. Compon., Packag., Manuf. Technol. **7**, 1395 (2017).
[23]E. Bardalen, B. Karlsen, H. Malmbekk, O. Kieler, M. N. Akram, and P. Ohlckers, Microelectron. Reliab. **81**, 362 (2018).
[24]O. Kieler, B. Karlsen, P. A. Ohlckers, E. Bardalen, M. N. Akram, R. Behr, J. Ireland, J. Williams, H. Malmbekk, L. Palafox, and R. Wendisch, IEEE Trans. Appl. Supercond. **29**, 1–8 (2019).
[25]B. Karlsen, O. Kieler, R. Behr, T. A. T. Nguyen, H. Malmbekk, M. N. Akram, and P. Ohlckers, IEEE Trans. Appl. Supercond. **29**, 1–5 (2019).
[26]F. Quinlan, S. Gee, S. Ozharar, and P. J. Delfyett, Opt. Lett. **31**, 2870 (2006).
[27]D. Kim, D. Kwon, B. Lee, and J. Kim, Opt. Lett. **44**, 1068 (2019).
[28]C. A. Donnelly, J. A. Brevik, P. D. Dresselhaus, P. F. Hopkins, and S. P. Benz, "Jitter sensitivity analysis of the superconducting Josephson arbitrary waveform synthesizer," IEEE Trans. Microwave Theory Tech. **66**, 4898–4909 (2018).
[29]T. Ishibashi, N. Shimizu, S. Kodama, H. Ito, T. Nagatsuma, and T. Furuma, "Uni-traveling-carrier photodiodes," in *Ultrafast Electronics and Optoelectronics*, edited by M. Nuss and J. Bowers (Optical Society of America, 1997), Vol. 13, p. 166.
[30]T. Kurokawa, T. Ishibashi, M. Shimizu, K. Kato, and T. Nagatsuma, Electron. Lett. **54**, 705 (2018).
[31]See https://www.albisopto.com/albis_product/pd20x1/ for a data sheet for "Albis Optoelectronics AG, Switzerland, PD20X1 28 Gb/s Photodiode With Integrated Lens."
[32]P.-L. Liu, K. J. Williams, M. Y. Frankel, and R. D. Esman, IEEE Trans. Microwave Theory Tech. **47**, 1297 (1999).
[33]See https://www.thorlabs.com/thorproduct.cfm?partnumber=BOA1132P for a data sheet for "Thorlabs BOA1132P Booster Amplifier."
[34]B. Baek, P. D. Dresselhaus, and S. P. Benz, IEEE Trans. Appl. Supercond. **16**, 1966 (2006).
[35]O. Kieler, R. Behr, D. Schleussner, L. Palafox, and J. Kohlmann, IEEE Trans. Appl. Supercond. **23**, 1301404 (2013).
[36]P. D. Dresselhaus, M. M. Elsbury, and S. P. Benz, IEEE Trans. Appl. Supercond. **19**, 993 (2009).
[37]W. C. Stewart, Appl. Phys. Lett. **12**, 277 (1968).
[38]D. E. McCumber, J. Appl. Phys. **39**, 2503 (1968).